



# Quantum Dynamics of Ultracold Na + Na<sub>2</sub> collisions

Pavel Soldán, Marko T. Cvitaš and Jeremy M. Hutson

*Department of Chemistry, University of Durham, South Road, Durham, DH1 3LE, England*

Pascal Honvault and Jean-Michel Launay

*UMR 6627 du CNRS, Laboratoire de Physique des Atomes, Lasers, Molécules et Surfaces, Université de Rennes, France*

(October 22, 2018)

Ultracold collisions between spin-polarized Na atoms and vibrationally excited Na<sub>2</sub> molecules are investigated theoretically, using both an inelastic formalism (neglecting atom exchange channels) and a reactive formalism (including atom exchange). Calculations are carried out on both pairwise additive and non-additive potential energy surfaces for the quartet electronic state. In both inelastic and reactive calculations, the Wigner threshold laws are followed for energies below 10<sup>-6</sup> K. It is found that vibrational relaxation processes dominate elastic processes for temperatures below 10<sup>-3</sup> – 10<sup>-4</sup> K. For temperatures below 10<sup>-5</sup> K, the rate coefficients for vibrational relaxation ( $v = 1 \rightarrow 0$ ) from the full calculation are  $4.8 \times 10^{-11}$  and  $5.2 \times 10^{-10}$  cm<sup>3</sup> s<sup>-1</sup> for the additive and non-additive potentials respectively.

Methods for creating diatomic molecules in atomic Bose-Einstein condensates (BECs) are now starting to be realised experimentally. They include photoassociation spectroscopy [1–4] and magnetic tuning through a Feshbach resonance [6,7]. An important long-range goal of such experiments is the production of a stable molecular BEC. However, in most cases the molecules are produced initially in vibrationally excited states, and their lifetime is limited by collisions with other atoms or molecules. Since the magnetic trap depth is typically 1 mK, any vibrationally or rotationally inelastic collision will release enough kinetic energy for both collision partners to be ejected from the trap.

Very little is known about vibrational relaxation rates for ultracold alkali dimers. Wynar *et al.* [2] produced <sup>87</sup>Rb<sub>2</sub> molecules in very high vibrational levels of the ground electronic state in an atomic BEC by stimulated Raman scattering. They analyzed their line shapes to obtain an upper bound on the inelastic rate coefficient  $k^{\text{inel}} < 8 \times 10^{-11}$  cm<sup>3</sup>/s. In subsequent experiments [5] on ultracold (but not condensed) Rb<sub>2</sub> molecules in a different set of vibrational levels, they measured  $k^{\text{inel}} = 3 \times 10^{-11}$  cm<sup>3</sup>/s. These rates are too high for the production of long-lived molecules, but there is a hope that lower-lying states will relax more slowly [8,10] and that methods for stabilizing the molecules can be found.

Several calculations have been carried out on the vibrational relaxation of molecules such as H<sub>2</sub> [8,10] and

CO [11,12] at ultralow energies. Spin-changing collisions of O<sub>2</sub> have also been investigated. [13,14] However, collisions of alkali dimers present new theoretical challenges that are not present for collisions of stabler molecules. In particular, the potential energy surfaces are such that barrierless atom-exchange reactions can occur; even if the products are indistinguishable from the reactants, the reactive channels must be taken into account in a full treatment of the collision dynamics. Barrierless reactions are significantly different from reactions such as F + H<sub>2</sub>, [15] which have substantial barriers, and have not yet been investigated at ultralow energies. This Letter presents an initial investigation of alkali + alkali dimer collisions, for the case of Na + Na<sub>2</sub> collisions occurring on the lowest quartet surface for Na<sub>3</sub>. This corresponds physically to collisions of atoms in their “stretched” spin states, with  $F = F_{\text{max}} = I + S$  and  $|M_F| = F$ .

In this work we use the potential energy surfaces of Higgins *et al.* [17] for the 1<sup>4</sup>A<sub>2</sub> state of Na<sub>3</sub>. Their full (non-additive) potential was obtained from a grid of *ab initio* calculations with a large basis set, interpolated using the reproducing-kernel Hilbert space scheme of Ho and Rabitz [18]. The potential has a global minimum at -1222.1 K, with the atoms in an equilateral triangle configuration 4.41 Å apart. The symmetric linear geometry is a saddle point at -554.4 K (667.7 K above the minimum), with  $r = 5.10$  Å. Comparison with the corresponding triplet Na<sub>2</sub> pair potential [19], which has  $r_e = 5.192$  Å and  $D_e = 255.7$  K, shows that large non-additive effects are present. In the present work, we test the sensitivity of our results to the potential surface by performing calculations using both the full non-additive potential and a potential obtained by neglecting the non-additive part.

We initially carried out inelastic scattering calculations of vibrational relaxation from the  $v = 1$  state of triplet Na<sub>2</sub>, using the MOLSCAT program [22]. Such calculations are carried out in Jacobi coordinates ( $R, r, \theta$ ) for a single arrangement of the atoms, and neglect the reactive channels. The wavefunction in the interaction region is expanded in a basis set of Na<sub>2</sub> vibrational functions that are eigenfunctions of the Hamiltonian for free Na<sub>2</sub>, supplemented by a wall at large  $R$  to provide a representation of the Na<sub>2</sub> continuum.

For full close-coupling or coupled states calculations, it proved impossible to converge the basis set of Na<sub>2</sub>

vibrational functions. This may readily be understood in terms of the potential energy surface. Consider Na approaching Na<sub>2</sub> for a T-shaped geometry,  $\theta = 90^\circ$ , allowing the Na<sub>2</sub> bond length  $r$  to relax to minimize the energy at each intermolecular distance  $R$ . The system passes through the minimum-energy equilateral geometry, and then the two atoms of the Na<sub>2</sub> move apart to allow the Na atom to insert between them. However, even at  $R = 0$  (the linear geometry), the energy is below that for separated Na + Na<sub>2</sub>. At this configuration, the optimum value of  $r$  is 10.4 Å, and the basis set of Na<sub>2</sub> vibrational functions centered around  $r_e = 5.1$  Å is completely inadequate for representing such dramatically expanded geometries.

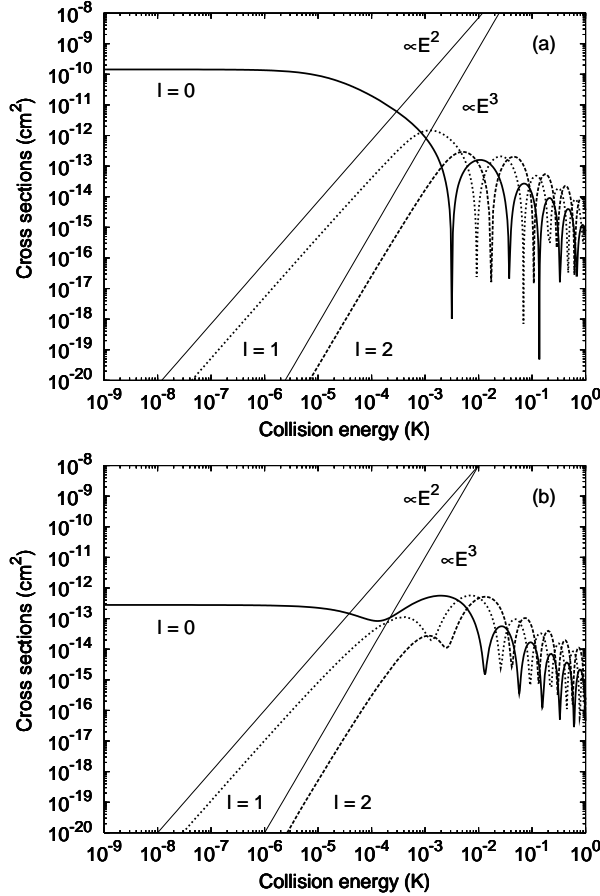


FIG. 1. Contributions to elastic cross sections from s, p and d waves for collinear Na + Na<sub>2</sub> ( $v = 1$ ) collisions, neglecting reactive channels. (a) additive potential. (b) non-additive potential.

This problem does not arise for collinear scattering, for which the vibrational basis set is adequately converged for  $v_{\max} = 20$ . We therefore carried out collinear calculations of the elastic and vibrational relaxation cross sections. The coupled equations were integrated from  $R = 2.3$  Å to 2500 Å. The resulting elastic and inelastic

cross sections for collisions of Na<sub>2</sub> initially in  $v = 1$  are shown in Figs. 1 and 2 for both the pairwise-additive and non-additive potentials.

The cross sections all follow the expected Wigner threshold laws [8,20,21] at energies below  $10^{-6}$  K. For elastic collisions, the cross sections are proportional to  $E^0$ ,  $E^2$  and  $E^3$  for s, p and d waves respectively. The  $E^3$  dependence for the d wave arises because the long-range dispersion ( $R^{-6}$ ) term in the atom-diatom potential modifies the threshold behavior for  $l > 1$  [21]. For vibrational relaxation, the cross sections are proportional to  $E^{-1/2}$ ,  $E^{1/2}$  and  $E^{3/2}$  for s, p and d waves respectively. The oscillations that occur for  $E > 1$  mK arise simply from zeroes in  $\sin^2 \eta$ , where  $\eta$  is the scattering phase shift.

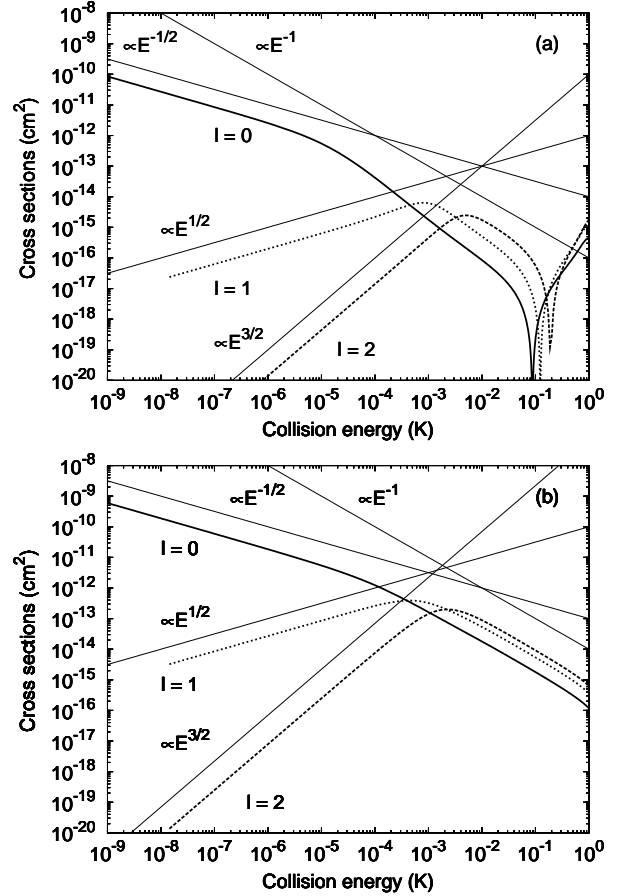


FIG. 2. Contributions to inelastic cross sections (to produce Na<sub>2</sub> ( $v = 1$ )) from s, p and d waves for collinear Na + Na<sub>2</sub> ( $v = 1$ ) collisions, neglecting reactive channels. (a) additive potential. (b) non-additive potential.

The *elastic* cross sections are dramatically different for the additive and non-additive potentials (by a factor of almost  $10^3$ ), while the *inelastic* cross sections are much more similar (differing by a factor of only 10). The large difference in the elastic cross sections presumably occurs because the zero-energy elastic cross section may be writ-

ten as  $\sigma_0^{\text{el}} = 4\pi|a|^2$ , where  $a$  is the atom-diatom complex scattering length [9]. This is accidentally close to zero for the non-additive potential:  $a = (-0.90 - 1.19i)$  nm, compared to  $(33.83 - 0.46i)$  nm for the additive potential. This has the effect that  $\sigma^{\text{el}} > \sigma^{\text{inel}}$  for  $T > 10^{-10}$  K on the additive surface, but only for  $T > 10^{-4}$  K on the non-additive surface.

An intriguing feature of the results is the appearance of a second linear region (in the log-log plots) for inelastic s-wave scattering between about  $10^{-5}$  and  $10^{-2}$  K. The cross section in this region is proportional to  $E^{-1}$  for the non-additive potential but to about  $E^{-4/3}$  for the additive potential. A possible reason for this is that the vibrational coupling at long range decays as  $R^{-6}$  for the full potential but as  $R^{-8}$  for the pairwise-additive potential.

As described above, the MOLSCAT calculations are restricted to collinear geometries and a single arrangement channel. To go beyond this requires a reactive scattering formalism in which all three arrangement channels are included. Such calculations are more expensive, and have not previously been attempted for systems containing three non-hydrogen atoms.

As a first step towards a rigorous treatment, we have performed three-dimensional quantum reactive scattering calculations for total nuclear orbital angular momentum  $J = 0$ . The configuration space is divided into an inner and an outer region, depending on the atom-diatom distance. In the inner region, we use a formalism based on body-frame democratic hyperspherical coordinates [23]. This has already proved successful in describing atom-diatom insertion reactions such as  $\text{N}(^2\text{D}) + \text{H}_2 \rightarrow \text{NH} + \text{H}$  [24] and  $\text{O}(^1\text{D}) + \text{H}_2 \rightarrow \text{OH} + \text{H}$  [25,26]. A related approach has also been used in studies of three-body recombination of ultracold atoms [27]. The scattering wave function is expanded on a set of hyperspherical adiabatic states. This yields a set of close-coupling equations, which in our method are solved using the Johnson-Manolopoulos log-derivative propagator [28]. In the outer region, we use the Arthurs-Dalgarno formalism [29], which is based on Jacobi coordinates. Matching of the wavefunctions in the inner and outer regions is performed on a boundary which is an hypersphere of radius 25 Å. This yields the reactance  $K$ -matrix and the scattering  $S$ -matrix.

The inner region starts at a hyperradius of 4 Å and is split into 297 sectors. The adiabatic states in each sector are obtained by a variational expansion on a basis of hyperspherical harmonics with  $A_1$  symmetry. They are fully symmetric with respect to particle permutations to account for the indistinguishability of atoms. At large hyperradius, the adiabatic states concentrate into the arrangement channels and describe  $\text{Na}_2$  molecules in even  $j$  states. At small hyperradius, they span a large fraction of configuration space and allow for atom exchange. The hyperspherical harmonic basis is truncated at  $\Lambda_{\text{max}}$ , the

maximum value of the grand angular momentum.  $\Lambda_{\text{max}}$  varies from 198 (867 harmonics) at small hyperradius to 398 (3400 harmonics) at large hyperradius. A fixed number of 135 adiabatic states is used in the close-coupling expansion in each sector. At the boundary between the inner and outer regions, the adiabatic states are projected onto a set of  $\text{Na}_2$  rovibrational states, with  $j_{\text{max}} = 48, 44, 40, 36, 30, 26, 20, 10$  for vibrational levels  $v = 0, 1, \dots, 7$ . The boundary between the inner and outer regions was placed at a distance such that couplings due to the atom-diatom residual interaction can be neglected outside the boundary. In the outer region, regular and irregular solutions of a radial Schrödinger equation which includes the isotropic ( $R^{-6}$ ) part of the interaction were integrated inwards from very large distances (5000 Å).

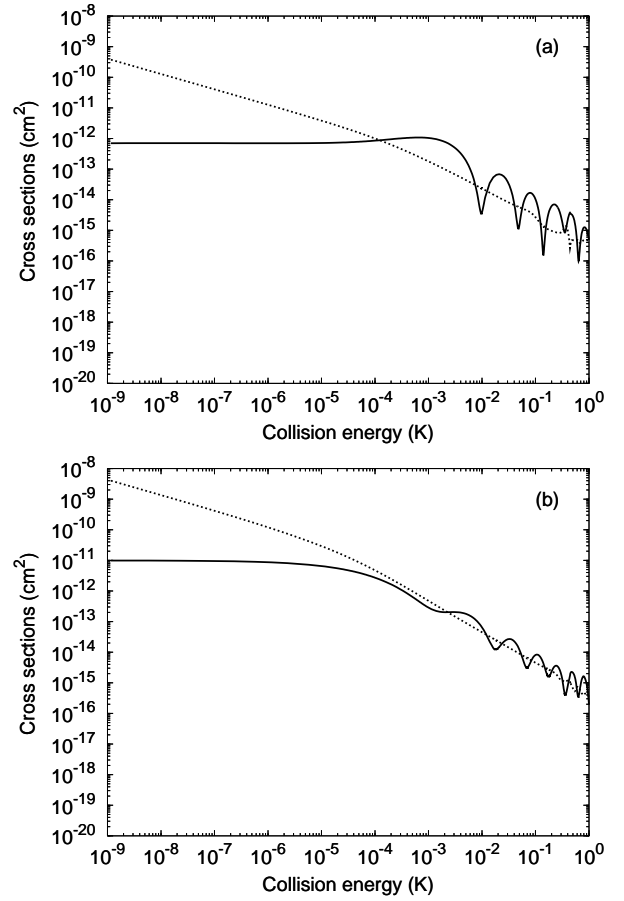


FIG. 3. Cross sections from quantum reactive scattering calculations for  $\text{Na} + \text{Na}_2(v = 1, j = 0)$  (s-wave scattering). Elastic and quenching results are shown as solid and dotted lines. (a) additive potential. (b) non-additive potential.

Fig. 3 shows the cross sections as a function of collision energy for the additive and non-additive potentials. All collisions that are energetically elastic, with or without atom exchange, are included in the elastic cross section. All other processes (which produce  $\text{Na}_2$  ( $v = 0, j$ )) con-

tribute to the quenching cross section.  $\text{Na}_2$  rotational levels up to  $j = 20$  are energetically accessible at the energy of the  $v = 1$  state ( $23.5 \text{ cm}^{-1}$ ), and all accessible levels are populated in the products.

It may be seen that the Wigner threshold laws for the elastic and quenching cross sections hold below  $10^{-5} \text{ K}$  for both potentials. The cross sections are larger for the non-additive than for the additive potential, by a factor of about 10 for both elastic and quenching cross sections. The  $E^{-1/2}$  dependence of the quenching cross sections corresponds to a constant rate coefficient below  $10^{-5} \text{ K}$ , which is  $k^{\text{inel}} = 4.8 \times 10^{-11} \text{ cm}^3 \text{ s}^{-1}$  for the additive potential and  $5.2 \times 10^{-10} \text{ cm}^3 \text{ s}^{-1}$  for the non-additive potential. The corresponding scattering lengths are  $a = (2.26 - 0.80i)$  and  $(2.38 - 8.54i) \text{ nm}$ , respectively.

Outside the Wigner region, the cross sections have a more complicated energy dependence. The quenching probability increases with increasing energy and approaches unity at the limit of the Wigner region. The quenching cross sections thus vary approximately as  $E^{-1}$  above  $10^{-4} \text{ K}$ , because of the  $k^{-2}$  factor in the expression for the cross section. Above  $10^{-3} \text{ K}$ , the elastic cross sections show oscillations which are similar to but less pronounced than the ones in Fig. 1.

Finally, the ratio of quenching to elastic cross sections is larger than 1 at energies below  $10^{-4} \text{ K}$  for the additive potential and below  $10^{-3} \text{ K}$  for the non-additive potential. It increases up to 500 in the nK range for both potentials.

In future work, we intend to investigate the dependence of quenching rates on the initial vibrational quantum number and to investigate the effects of magnetic fields and nuclear spin coupling.

The three-dimensional quantum dynamical calculations were performed on a NEC-SX5 vector supercomputer, through a grant from the “Institut du Développement des Ressources en Informatique Scientifique” (IDRIS) in Orsay (France). PS is grateful to the EPSRC for a Research Associateship under grant no. GR/R17522/01.

- 
- [1] W. C. Stwalley and H. Wang, *J. Mol. Spectrosc.* **195**, 194 (1999).
  - [2] R. Wynar, R. S. Freeland, D. J. Han, C. Ryu, and D. J. Heinzen, *Science* **287**, 1016 (2000).
  - [3] J. M. Gerton, D. Strelakov, I. Prodan and R. G. Hulet, *Nature* **408**, 692 (2000).
  - [4] C. McKenzie, J. H. Denschlag, H. Häffner, A. Browaeys, *et al.*, *Phys. Rev. Lett.* **88**, 120403 (2002).
  - [5] D. J. Heinzen *et al.*, unpublished work.
  - [6] F. H. Mies, E. Tiesinga and P. S. Julienne, *Phys. Rev. A* **61**, 022721 (2000).
  - [7] E. A. Donley, N. R. Claussen, S. T. Thompson and C. E. Wieman, *Science*, submitted. (available at <http://lanl.arxiv.org/abs/cond-mat/0204436>)
  - [8] N. Balakrishnan, R. C. Forrey, and A. Dalgarno, *Chem. Phys. Lett.* **280**, 1 (1997).
  - [9] N. Balakrishnan, V. Kharchenko, R. C. Forrey, and A. Dalgarno, *Chem. Phys. Lett.* **280**, 5 (1997).
  - [10] N. Balakrishnan, R. C. Forrey, and A. Dalgarno, *Phys. Rev. Lett.* **80**, 3224 (1998).
  - [11] N. Balakrishnan, A. Dalgarno, and R. C. Forrey, *J. Chem. Phys.* **113**, 621 (2000).
  - [12] C. Zhu, N. Balakrishnan and A. Dalgarno, *J. Chem. Phys.* **115**, 1335 (2001).
  - [13] J. L. Bohn, *Phys. Rev. A* **62**, 032701 (2000).
  - [14] A. V. Avdeenkov and J. L. Bohn, *Phys. Rev. A* **64**, 052703 (2001).
  - [15] N. Balakrishnan and A. Dalgarno, *Chem. Phys. Lett.* **341**, 652 (2001).
  - [16] N. Balakrishnan and A. Dalgarno, *Chem. Phys. Lett.* **341**, 652 (2001).
  - [17] J. Higgins, T. Hollebeek, J. Reho, T.-S. Ho, K. K. Lehmann, H. Rabitz, and G. Scoles, *J. Chem. Phys.* **112**, 5751 (2000).
  - [18] T.-S. Ho and H. Rabitz, *J. Chem. Phys.* **104**, 2584 (1996).
  - [19] M. Gutowski, *J. Chem. Phys.* **110**, 4695 (1999).
  - [20] E. P. Wigner, *Phys. Rev.* **73**, 1002 (1948).
  - [21] H. R. Sadeghpour, J. L. Bohn, M. J. Cavagnero, B. D. Esry, I. I. Fabrikant, J. H. Macek, and A. R. P. Rau, *J. Phys. B: At. Mol. Opt. Phys.* **33**, R93 (2000).
  - [22] J. M. Hutson and S. Green, MOLSCAT computer program, version 14, distributed by Collaborative Computational Project No. 6 of the UK Engineering and Physical Sciences Research Council, 1994. Some modifications were made to improve the efficiency for ultracold collisions.
  - [23] J.-M. Launay and M. Le Dourneuf, *Chem. Phys. Lett.* **163**, 178 (1989).
  - [24] P. Honvault and J.-M. Launay, *J. Chem. Phys.* **111**, 6665 (1999).
  - [25] P. Honvault and J.-M. Launay, *J. Chem. Phys.* **114**, 1057 (2001).
  - [26] F. J. Aoiz, L. Bañares, J. F. Castillo, M. Brouard, W. Denzer, C. Vallance, P. Honvault, J.-M. Launay, A. J. Dobbyn and P. J. Knowles, *Phys. Rev. Lett.* **86**, 1729 (2001).
  - [27] B. D. Esry, C. H. Greene and J. P. Burke, Jr., *Phys. Rev. Lett.* **83**, 1751 (1999).
  - [28] D.E. Manolopoulos, *J. Chem. Phys.* **85**, 6425 (1986).
  - [29] A.M. Arthurs and A. Dalgarno, *Proc. R. Soc. A* **256**, 540 (1960).